ELSEVIER

Journal of Alloys and Compounds 468 (2009) 280–284

Journal of ALLOYS AND COMPOUNDS

www.elsevier.com/locate/jallcom

Pressure-induced spin and charge transport in $La_{1.25}Sr_{1.75}Mn_2O_7$ single crystal

K. Mydeen [a,b,*], S. Arumugam [b], D. Prabhakaran [c], R.C. Yu [a], C.Q. Jin [a]

[a] *Beijing National Laboratory for Condensed Matter Physics, Institute of Physics, Chinese Academy of Sciences, Beijing 100080, China*
[b] *HPLT Laboratory, School of Physics, Bharathidasan University, Tiruchirappalli 620024, India*
[c] *Department of Physics, Clarendon Laboratory, University of Oxford, Oxford OX1, United Kingdom*

Received 18 September 2007; received in revised form 17 December 2007; accepted 20 December 2007
Available online 3 January 2008

Abstract

We investigated the effect of uniaxial and hydrostatic pressure on resistivity and ac-magnetic susceptibility of two-dimensional layered manganite, $La_{1.25}Sr_{1.75}Mn_2O_7$ (LSMO125) to investigate the lattice effect on magnetic and electronic properties. Asymmetric role of uniaxial pressure, || and ⊥ to *c*-axis on the spin flop and charge transport has been revealed while comparing hydrostatic pressure. Uniaxial pressure along *c*-axis increases metal–insulator transition temperature (T_{MI}) and ferromagnetic ordering temperature (T_C), whereas it decreases the resistivity along ab-plane (ρ_{ab}). In contrast to pressure along *c*-axis, T_{MI} and T_C decrease, whereas the resistivity along *c*-axis (ρ_c) increases with pressure || to ab-plane. ρ_c/ρ_{ab} is quite large, increasing with pressure and shows a peak at around T_{MI}. Uniaxial pressure behaviour is strongly related to the Mn–O–Mn linkage between MnO_2 layers and the spin reorientation from the apical axis to the basal plane and vice versa with pressure. Both ρ_{ab} and ρ_c decrease whereas T_{MI} and T_C increases under hydrostatic pressure. Influence of spin and charge on magnetic and electrical properties under hydrostatic pressure are explained by pressure-induced cant between the MnO_2 bilayers and variation in bond lengths. The different pressure driving rates of T_{MI} while measuring ρ_{ab} and ρ_c confirms that there is a strong competition between the in and out plane components under hydrostatic pressure.

PACS: 74.62.Fj; 74.25.Fy; 74.25.Ha

Keywords: Uniaxial pressure; Hydrostatic pressure; Electrical properties; Magnetic properties

1. Introduction

The discovery of colossal magnetoresistance (CMR) effect in low-dimensional manganites with perovskite structure has attracted the considerable interest for the understanding of their unrevealed physical properties [1]. CMR in the doped manganites is related to a temperature-dependent phase transition that occurs from a paramagnetic insulator to a ferromagnetic metal. Just above this transition, an applied magnetic field not only restores the magnetic phase but also stabilizes the metallic state. Though the insulator-to-metal transition and its associated CMR properties are well explained on the basis of the double-exchange (DE) model, it is to be considered that the dynamic Jahn–Teller (JT) effect due to the strong electron–phonon interaction, plays a key role in the appearance of CMR as well as the DE interaction [2,3]. In bilayer manganites $La_{2-2x}Sr_{1+2x}Mn_2O_7$, MnO_2 conducting bilayer is alternatively stacked with a $(La,Sr)_2O_2$ insulating rock-salt blocking layer along the *c*-axis. As a consequence, bilayer manganites show highly anisotropic transport properties with the magnitude of resistivity along the *c*-axis about two or more orders higher than that along the ab-plane, extremely large interplane tunneling magnetoresistance, and a reduced Curie temperature [4]. Another important feature of this system is that the interlayer tunneling conduction is extremely sensitive to external pressure and hole doping (x) [5]. For $x = 0.30$, both ρ_c and ρ_{ab} increase dramatically with hydrostatic pressure up to 1.4 GPa [6], but for $x = 0.32$ resistivity along both directions decreases with the hydrostatic pressure up to 1.8 GPa [7]. For both $x = 0.3$ and 0.32 one can find the ferromagnetic order within the bilayer and 3D ferromagnetic alignment

* Corresponding author at: Beijing National Laboratory for Condensed Matter Physics, Institute of Physics, Chinese Academy of Sciences, Beijing 100080, China. Tel.: +86 10 82649160; fax: +86 10 82649163.
E-mail address: kmydeen@aphy.iphy.ac.cn (K. Mydeen).

0925-8388/$ – see front matter © 2008 Elsevier B.V. All rights reserved.
doi:10.1016/j.jallcom.2007.12.076

between the bilayers for $0.4 > x > .0.32$. In the case of $x = 0.30$, the weak interbilayer coupling is antiferromagnetic (AF), producing an A-type AF ground state with moments aligned along the *c*-axis [8]. Investigations over the structural studies on bilayer manganites have revealed that the compressibility along the *c*-axis is different from that along the ab-plane [9]. Particularly *c*-axis Mn–O(1) and Mn–O(2) bond lengths show the reciprocal response to temperature and pressure which reflects the asymmetric *c*-axis bonding at a Mn atom and Mn–O(2) bonds are free to adjust their length for retaining the equilibrium bond length sum for the Mn valences. It has also been proved that there is *a*-axis compressibility by the reduction of the Mn–O(3) bond length and no change in Mn–O(3)–Mn bond angle which indicates no additional buckling of MnO_6 octahedra occurring with applied pressure. This is in contrast to other perovskite materials [10,11]. We believe that the effect of uniaxial pressure on transport properties would be very different from that of hydrostatic pressure hence the bilayer manganites show the strong anisotropic structural, electronic, and magnetic coupling. Our previous report about the uniaxial pressure effect on electrical resistivity reveals the importance of the lattice parameter over the transport properties [12]. To the best of our knowledge, there are no such reports on ac-magnetic susceptibility under uniaxial pressure in bilayer manganites up to now. By keeping these positive remarks in mind, we have studied the followings: (1) ab-plane and *c*-axis resistivities with pressure always perpendicular to the direction of the flow of current. (2) ab-plane and *c*-axis ac-susceptibilities with pressure and weak ac-field parallel to each other. We also studied ab-plane and *c*-axis resistivities and susceptibilities with hydrostatic pressure up to 2 GPa for comparison.

2. Experimental details

High quality single crystal samples are indispensable for experimental investigations of the mechanisms related to the CMR effect. Single crystals with nominal composition $La_{1.25}Sr_{1.75}Mn_2O_7$ (LSMO125) were grown from polycrystalline rods using an optical floating-zone furnace in a controlled atmosphere because of its high melting temperature [13]. Different experimental techniques were adopted to confirm the phase purity, structure, and crystalline quality. The nature of the crystal surface was checked by optical and scanning electron microscopy. X-ray powder diffraction reveals high purity of the phase, and the sharp diffraction spots in Laue diffraction indicate good crystalline quality. The elemental analysis was done using electron probe microanalysis and found to be very close to the nominal composition. The magnetic properties were studied by a superconducting quantum interference device (SQUID) magnetometer (Quantum Design) with a small field applied parallel and perpendicular to the ab-plane. Both field-cooled (FC) and zero-field-cooled (ZFC) magnetization measurements show a sharp ferromagnetic transition close to the metal–insulator transition (T_{MI}) at ~128 K. All these measurements clearly show that our single crystals are of high quality. Well characterized crystals were aligned with a goniometer using Laue back diffraction pattern and cut along the ab-plane and *c*-axis with typical dimensions 1 mm × 1 mm × 1 mm using diamond wire cutter and all the faces were polished finely using Al_2O_3 (50 nm) powder with water.

2.1. Uniaxial pressure technique

The temperature dependence of DC resistivity under uniaxial pressure in zero field ($\rho(T,P)$) was measured by van der Pauw geometry [14] with the current between 10 and 100 μA using a simple uniaxial pressure device specially designed for electrical resistivity measurements suitable for closed cycle refrigerator system [15]. Electrical resistivity measurements under uniaxial pressure were performed on highly polished samples prepared by epoxy crystal bare surface (ECBS) technique [16]. ECBS samples were placed in between the anvils made of Be (2%)–Cu alloy. The surfaces of the anvils were electrically insulated by introducing the fine layer of GE varnish (GE 7031). The pads for electrical contacts on the samples were made by Au paint and then annealed at an appropriate temperature. The details about the sample mounting techniques has been published elsewhere [15]. Temperature dependence of ac-susceptibility measurements under uniaxial pressure were also performed on the samples from the same batch using a home-built ac-susceptometer with uniaxial pressure device specially designed for ac-magnetic susceptibility measurements [16] under an ac-probe field of ≈2 Oe and an excitation frequency of 133 Hz. The in-phase component of ac-susceptibility (χ') alone considered for further discussion as (χ'') is negligibly small. In case of ac-magnetic susceptibility measurements under uniaxial pressure, the similar procedures were followed like resistivity measurements under uniaxial pressure. The same ECBS sample preparation technique were adopted to prepare the sample for magnetic studies and the prepared sample were mounted in between the suitable Be (2%)–Cu anvils, which was inserted into the suitable former-coil assembly for magnetic studies, details about the sample mounting techniques have been published elsewhere [16]. Cernox (CX-1030) magnetic free sensors were used for measuring the temperature with the accuracy of 0.2 K. In this device pressure was applied through a force generator by rotating a micrometer and the pressure was calculated directly from the surface area of the crystal, the rotations of the micrometer, and the force-constant value of the spring.

2.2. Hydrostatic pressure technique

A self-clamp type hybrid double cylinder (nonmagnetic Ni–Cr–Al inner cylinder; Be–Cu outer cylinder) pressure cell was used to generate various hydrostatic pressures up to 2 GPa, which was monitored using a manganin resistance device. The mixture of fluorinate FC70:FC77 was used as a pressure-transmitting medium. The temperature variation was monitored using a chromel–constantan thermocouple calibrated for the pressure-induced changes placed near the sample (inside the Teflon capsule). Pressure decreased continuously with the lowering of temperature at the average rate of 0.0013 GPa/K from 300 to 77 K. The values of various pressures appearing in this manuscript refer to the values measured at room temperature and the data to be considered here are during warming process only.

3. Results and discussion

The temperature dependence of ρ_{ab} with pressure || to *c*-axis and ρ_c with pressure ⊥ to *c*-axis at different uniaxial pressures (*P*) are shown in Fig. 1(a) and (b), respectively. At ambient pressure and temperature the electrical resistivity is highly anisotropic with $\rho_c/\rho_{ab} \sim 60$ (not shown), which is comparable with earlier reports [6,7]. Both ρ_{ab} and ρ_c increase with the decrease of temperature and exhibit an insulator-to-metal transition at T_{MI} 128 ± 0.5 K. The temperature dependence of FC and ZFC magnetization (*M*) shows that *M* increases sharply just below T_{MI} [12] and T_{MI} coincides with T_C. With increasing *P*, ρ_{ab} decreases and T_{MI} shifts monotonically towards higher temperature. The effect of *P* on reducing ρ_{ab} is stronger close to the vicinity of T_{MI}. In contrast to ρ_{ab}, ρ_c increases sharply with increasing pressure, T_{MI} shifts towards lower temperature, and the effect of pressure is stronger and extended over a much wider range of temperature both above and below T_{MI}. Neglecting the weak nonlinear dependence of T_{MI} on *P*, we find that for *P* || to *c*-axis, T_{MI} increases at a rate (dT_{MI}/dP) of 46.33 K/GPa while T_{MI} decreases at a rate of 16.58 K/GPa, for *P* ⊥ to *c*-axis. The rate of increase of T_{MI} in LSMO125 under uniaxial pressure is comparable to 38 K/GPa in $La_{1.36}Sr_{1.64}Mn_2O_7$ under hydro-

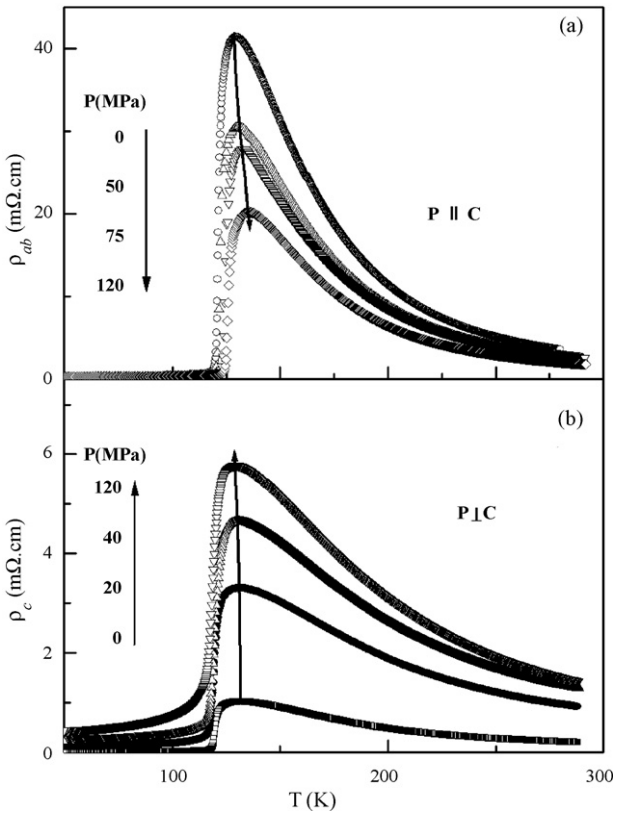

Fig. 1. Temperature dependence of (a) ρ_{ab} with pressure || to c-axis and (b) ρ_c with pressure ⊥ to c-axis of $La_{1.25}Sr_{1.75}Mn_2O_7$. The arrows indicate the direction of metal–insulator transition temperature shift.

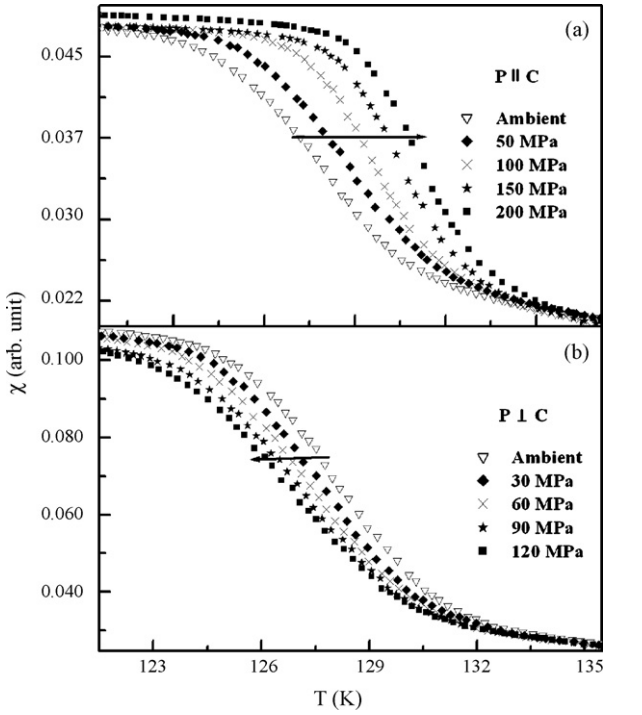

Fig. 2. Temperature dependence of ac-susceptibility at different uniaxial pressures: (a) || to c-axis and (b) ⊥ to c-axis $La_{1.25}Sr_{1.75}Mn_2O_7$. The arrows indicate the direction of ferromagnetic ordering temperature shift.

static pressure but much higher than that observed in perovskite manganites $La_{3/4}Ca_{1/4}MnO_3$ (10 K/GPa). The results obtained for the T dependence of the ac-susceptibility, at different uniaxial pressures || and ⊥ to c-axis are presented in Fig. 2(a) and (b), respectively. The sample exhibits a very sharp paramagnetic (PM)–ferromagnetic (FM) transition at the Curie temperature (T_C). We have defined the inflection point of the χ–T curve as T_C 128 ± 0.5 K, at ambient pressure, which is comparable with the previous results [12]. With increasing pressure || to c-axis the T_C increases at the rate of 18.2 ± 0.2 K/GPa, in contrast to pressure || to c-axis, T_C decreases at the rate of 10.03 ± 0.2 K/GPa with the application of pressure ⊥ to c-axis. Temperature dependence of ac-susceptibility is weak at $T > T_C$ for both direction of uniaxial pressure || and ⊥ to c-axis. Fig. 3(a) and (b) shows the temperature dependence of ρ_{ab} and ρ_c of the LCMO125 under different hydrostatic pressures. It is found that, with decreasing temperature both ρ_c and ρ_{ab} are increased and showed a sharp maximum at temperature, T_{MI} 128 ± 0.5 K. When the temperature is further decreased below T_{MI}, both ρ_{ab} and ρ_c are decreased. Hydrostatic pressure suppress ρ_{ab} and ρ_c monotonically through out the whole range of measurement. Considering the near linear response of T_{MI} while measuring ρ_{ab} and ρ_c under hydrostatic pressure, it is observed that pressure shifts T_{MI} to higher temperatures with pressure coefficients 14.6 ± 0.2 K/GPa and 8.2 ± 0.2 K/GPa, respectively, which are comparable with the previous results [17]. Fig. 4(a) and (b) shows the temperature dependence of χ_{ab} and χ_c for LCMO125 under hydrostatic pres-

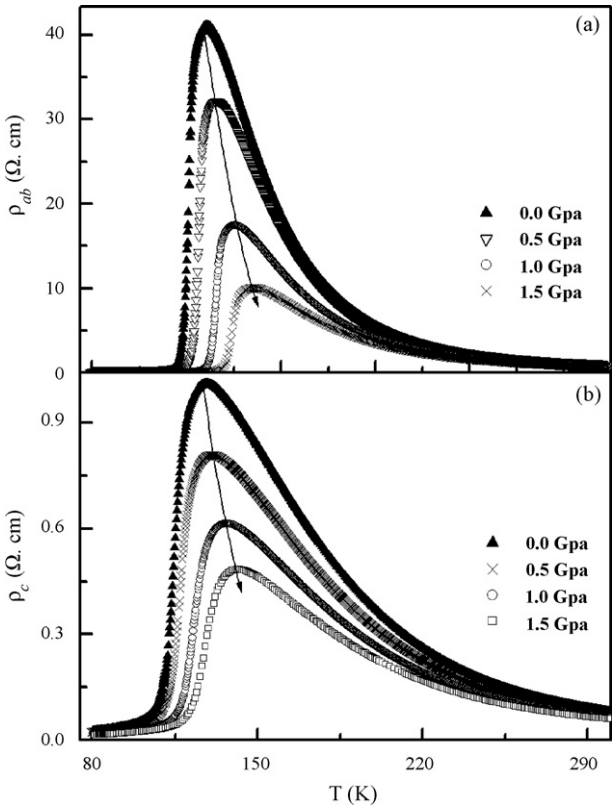

Fig. 3. Temperature dependence of (a) ρ_{ab} and (b) ρ_c of $La_{1.25}Sr_{1.75}Mn_2O_7$ under different hydrostatic pressures. The arrows indicate the direction of metal–insulator transition temperature shift.

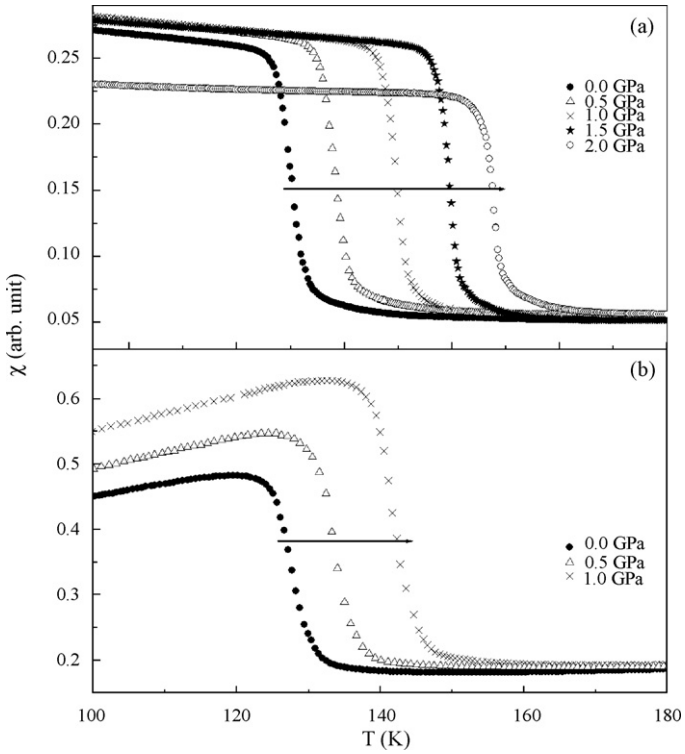

Fig. 4. Temperature dependence of (a) χ_{ab} [ab-plane || to ac-field] and (b) χ_c [ab-plane $\perp$ to ac-field] of $La_{1.25}Sr_{1.75}Mn_2O_7$ under different hydrostatic pressures. The arrows indicate the direction of ferromagnetic ordering temperature shift.

sure. It is observed that a sharp transition occurs at $\sim 128 \pm 0.5$ K, which represents the paramagnetic to ferromagnetic ordering at ambient pressure. T_C increases with pressure coefficients of $dT_C/dP = 14.1 \pm 0.2$ K/GPa and $dT_C/dP = 11.9 \pm 0.2$ K/GPa while keeping c-axis $\perp$ and || to the weak applied ac-field, respectively.

At ambient pressure, the electrical and magnetic properties of LSMO125 can be basically understood on the basis of double exchange (DE) interaction theory [18,19]. According to this theory, these manganese oxide compounds have Mn^{3+} and Mn^{4+} ions and these ionic states fluctuate due to electron transfer between them. As a result of this electron transfer manganese spins cant, and both magnetization and metallic conductivity appear simultaneously. The magnetization increases as the canting angle decreases. LSMO125 shows the ferromagnetic order within the bilayer and 3D ferromagnetic alignment between the bilayers in ground state [8]. Neutron diffraction experiments on $La_{1.2}Sr_{1.8}Mn_2O_7$ (LSMO12) single crystals reveal that the MnO_6 octahedra in the layered manganite undergoes enhanced distortion in the metallic regime where the charge is delocalized through the double-exchange mechanism [20]. The two-layer structure appears to accommodate the pressure effects through the change in Mn–O bond lengths rather than by the tilting of the MnO_6 octahedra under pressure, which happens in the perovskite oxide. A general feature of all those layered compounds is the fact that the interbilayer coupling is orders of magnitudes smaller than the intrabilayer coupling. The electrical anomaly bound to the metal–insulator transition shifted by pressure is different with the magnetic anomaly. The structural response due to external pressure leads to modifying the electronic transfer integral between Mn–Mn. It has been recently proved that the electronic and magnetic transitions of many manganites may be significantly decoupled, especially under hydrostatic pressure [21]. Therefore, the applied pressure affects the different conduction channels and in turn results in the variation of T_{MI} and T_C.

To interpret the unusual uniaxial pressure dependence of resistivity and ac-susceptibility while comparing hydrostatic pressure response we must be accountable for the followings: (1) the magnitude of the interlayer charge and spin couplings are highly sensitive to pressure; (2) the electronic and spin coupling along c-axis is very weak due to the presence of the insulating rock salt-type $(La,Sr)_2O_2$ layers in the conducting MnO_2 layers; (3) in-plane compressibility is smaller than the interplane compressibility; (4) effect of uniaxial pressure on the spin and charge transfer is stronger than the applied weak magnetic field; (5) effect of hydrostatic pressure on the spin and charge transfer is the result of the competition between the in and out plane components. While measuring ρ_{ab} and ac-susceptibility with pressure along the c-axis, the apical Mn–O bond length gets compressed and as a result the system anisotropy is reduced monotonically. Also, the shorter apical Mn–O bond favors the flop of the spins and charge transfer from the apical axis to the conduction plane, further pressure applying along the apical axis increases the strength of coupling between and within the conducting MnO_2 layers. All these effects enhance the in-plane conductivity of the system and T_C. In contrast, the increase of ρ_c and the decrease of T_{MI} as well as T_C with pressure along the ab-plane can be explained by considering the effect of small expansion along the c-axis due to the Poisson ratio. In this case the pressure enhances the in-plane coupling along the direction of the applied pressure but reduces the interlayer linkage due to the expansion along the c-axis. As the coupling between the planes is very weak and the conductivity along the c-axis is due to the tunneling of charge carriers, a small increase in the apical Mn–O bond length may suppress the conductivity due to the in-plane compression. The small increase of the c-axis Mn–O–Mn bond length may also change the spin orientation from the basal plane to c-axis. This effect will further reduce the conductivity in the vicinity of T_C and T_{MI}, and increase the anisotropy of the system. On the other hand, both magnetic and electronic couplings between the layers are responsible for the sharp increase of the anisotropy at T_C and T_{MI} [12]. The different pressure driving rate of T_{MI} and T_C confirms that the electronic and magnetic anomaly induced by uniaxial pressure is different.

It is to be highlighted that the decrease in the interbilayer spacing and the shift of the Mn atoms away from the center of each bilayer result in increased magnetic and electronic coupling between the adjacent bilayers along the c-axis, which can be effectively tuned by the external hydrostatic pressure. In the absence of magnetic order in the PI state, there is no spin–spin repulsion, and pressure increases the overlap integrals to give a normal reduction of the equilibrium Mn–O bond lengths within and between the MnO_2 sheets, also in the FM state the Mn–O–Mn linkage between MnO_2 layers expands under

hydrostatic pressure [22]. This makes the FM state more and more anisotropic with pressure and leads to increase the T_C and drop the resistance effectively. Increasing hydrostatic pressure reducing the cant angle between the MnO_2 sheets and leads to the positive dT_C/dP. Under hydrostatic pressure temperature dependence of ρ_c is so strong in the vicinity of T_{MI} in comparison with ρ_{ab}, which suggests that the transport properties are very sensitive to small change in apical Mn–O bond length. Increasing pressure broadens ρ_{ab} and ρ_c in the vicinity of T_{MI}, which provides the evidence of the stabilization of 2D like conduction. The different pressure driving rates of T_{MI} for ρ_{ab}, and ρ_c confirms that there is a strong competition between in and out plane components.

4. Conclusions

In summary, we have studied the temperature dependence of uniaxial and hydrostatic pressure effects on resistivity and ac-susceptibility in single crystals of the bilayer manganite $La_{1.25}Sr_{1.75}Mn_2O_7$. With increasing uniaxial pressure along the *c*-axis, ρ_{ab} decreases whereas T_{MI} and T_C shifts towards higher temperature due to the enhancement of the interlayer coupling and spin flop from *c*-axis to conduction plane. On the other hand, the application of uniaxial pressure along the ab-plane reduces the interlayer coupling, and as a result ρ_c increases whereas T_{MI} and T_C decreases. Application of hydrostatic pressure, decreases ρ_{ab} and ρ_c whereas T_{MI} and T_C shifts to the higher temperature. Increasing hydrostatic pressure leads to stabilize the 2D like conduction in LCMO125. The electronic and magnetic anomaly tuned by the uniaxial and hydrostatic pressure is highly sensitive to pressure.

Acknowledgements

The author would like to thank the Third World Academy of Sciences, Italy and Chinese Academy of Sciences, China for the award of CAS-TWAS fellowship. This work was partially supported by NSF & MOST of China through the research projects.

References

[1] Y. Tokura (Ed.), Colossal Magnetoresistive Oxides, Gordon and Breach, New York, 2000.
[2] C. Zener, Phys. Rev. 82 (1951) 403.
[3] A.J. Millis, P.B. Littlewood, B.I. Shraiman, Phys. Rev. Lett. 74 (1995) 5144.
[4] T. Kimura, Y. Tomioka, H. Kuwahara, A. Asamitsu, M. Tamura, Y. Tokura, Science 274 (1996) 1698.
[5] K. Hirota, Y. Moritomo, H. Fujioka, M. Kubota, H. Yoshizawa, Y. Endoh, J. Phys. Soc. Jpn. 67 (1998) 3380.
[6] T. Kimura, A. Asamitsu, Y. Tomioka, Y. Tokura, Phys. Rev. Lett. 79 (1997) 3720.
[7] J.-S. Zhou, J.B. Goodenough, J.F. Mitchell, Phys. Rev. B 61 (2000) R9217.
[8] A. Berger, J.F. Mitchell, D.J. Miller, J.S. Jiang, S.D. Bader, J. Vac. Sci. Technol. A 18 (2000) 1239.
[9] D.N. Argyriou, J.F. Mitchell, J.B. Goodenough, O. Chmaissem, S. Short, J.D. Jorgensen, Phys. Rev. Lett. 78 (1997) 1568.
[10] Y. Zhao, D.J. Weidner, J.B. Parise, D.E. Cox, Phys. Earth Planet. Inter. 76 (1993) 17.
[11] J.-E. Jorgensen, J.D. Jorgensen, B. Batlogg, J.P. Remeika, J.D. Axe, Phys. Rev. B 33 (1986) 4793.
[12] S. Arumugam, K. Mydeen, N. Manivannan, M. Kumaresa Vanji, D. Prabhakaran, A.T. Boothroyd, R.K. Sharma, P. Mandal, Phys. Rev. B 73 (2006) 212412.
[13] D. Prabhakaran, A.T. Boothroyd, J. Mater. Sci.: Mater. Electron. 14 (2003) 587.
[14] van der Pauw Philips Res. Rep. 13 (1958) 1.
[15] S. Arumugam, K. Mydeen, M. Kumaresa Vanji, N. Mori, Rev. Sci. Instrum. 76 (2005) 083904.
[16] K. Mydeen, S. Arumlugam, Y. Yuang, C.Q. Jin, CPL. communicated.
[17] S. Arumugam, K. Mydeen, M. Fontes, N. Manivannan, M Kumaresa Vanji, K.U. RamaTulasi, S.M. Ramos, E.B. Saitovitch, D. Prabhakar, A.T. Boothroyd, J. Solid State Commun. 136 (2005) 292.
[18] P.W. Anderson, H. Hasegawa, Phys. Rev. 100 (1995) 675.
[19] P.G. de Gennes, Phys. Rev. 118 (1960) 141.
[20] J.F. Mitchell, D.N. Argyriou, J.D. Jorgensen, D.G. Hinks, C.D. Potter, S.D. Bader, Phys. Rev. B 55 (1992) 63.
[21] C. Cui, T.A. Tyson, Phys. Rev. B 70 (2004) 094409.
[22] K.V. Kamenev, M.R. Lees, G. Balakrishnan, C.D. Dewhurst, D.McK. Paul, Physica B 265 (1999) 191.